View metadata, citation and similar papers at core.ac.uk

brought to you by CORE

provided by Publications of the IAS Fellows

Ge growth on ion-irradiated Si self-affine fractal surfaces

D. K. Goswami, K. Bhattacharjee and B. N. Dev*

Institute of Physics, Sachivalaya Marg, Bhubaneswar -751005, India

(Dated: February 2, 2008)

arXiv:cond-mat/0403241v1 [cond-mat.mtrl-sci] 9 Mar 2004

We have carried out scanning tunneling microscopy experiments under ultrahigh vacuum condition to study the morphology of ultrathin Ge films deposited on pristine Si(100) and ion-irradiated Si(100) self-affine fractal surfaces. The pristine and the ion-irradiated Si(100) surface have roughness exponents of $\alpha = 0.19 \pm 0.05$ and $\alpha = 0.82 \pm 0.04$ respectively. These measurements were carried out on two halves of the same sample where only one half was ion-irradiated. Following deposition of a thin film of Ge ($\sim 6\AA$) the roughness exponents change to 0.11±0.04 and 0.99±0.06, respectively. Upon Ge deposition, while the roughness increases by more than an order of magnitude on the pristine surface, a smoothing is observed for the ion-irradiated surface. For the ion-irradiated surface the correlation length ξ increases from 32 nm to 137 nm upon Ge deposition. Ge grows on Si surfaces in the Stranski-Krastanov or layer-plus-island mode where islands grow on a wetting layer of about three atomic layers. On the pristine surface the islands are predominantly of square or rectangular shape, while on the ion-irradiated surface the islands are nearly diamond shaped. Changes of adsorption behaviour of deposited atoms depending on the roughness exponent (or the fractal dimension) of the substrate surface are discussed.

PACS numbers: 68.35.Ct; 61.80.Jh; 68.55.Jk; 68.37.Ef
Keywords: Ion-irradiation induced fractal surfaces, Thin film growth on fractal surfaces, Scaling, Scanning tunneling microscopy

I. INTRODUCTION

A wide variety of surfaces are present in nature where surface roughness is well described in terms of self-affine fractal scaling spanning various length scales – for example, the kilometer-scale structure of mountain terrain [1] to nanometer-scale topology of thin films obtained by deposition of atoms or molecules on substrates [2] and of ion-bombarded surfaces [3, 4, 5]. Various physical processes including fracture, ion bombardment, molecular beam epitaxy etc. produce this kind of surface morphology. In thin film deposition the morphology of the bare surfaces of substrates prior to thin film deposition can also influence the morphology of the deposited films. To a large extent the usefulness of thin films in terms of mechanical, optical and electrical properties depends on the surface morphology. It is important to understand growth mechanisms leading to various surface morphologies.

Ion irradiation and molecular beam epitaxy (MBE) – both used in advanced modern technology – affect surface morphologies in different ways. In the case of heteroepitaxial MBE growth there are three different growth modes – layer-by-layer (Frank-van der Merwe or FM), island (Volmer-Weber or VW) and layer-plus-island (Stranski-Krastanov or SK) [6]. Thus MBE growth can produce different surface morphologies. Which growth mode will be adopted in a given system depends on the surface free energy of the substrate, free energy of the film, their interface energy and the strain energy due to lattice mismatch. Thus the surface morphology is governed by these parameters. Ion bombardment produces rough surface as well as smooth surface under different experimental conditions. A common feature of most of the ion-bombarded surfaces is self-affine fractal structure. The fractal dimensions of such self-affine surfaces can be controlled. The adhesion of a thin film deposited on a fractal surface is expected to be affected by the fractal dimension of the substrate surface [7]. This inspires studies of the morphology of MBE-grown thin films on ion-irradiated substrates. Here we report our results of such studies and compare the growth on pristine and ion-irradiated surfaces.

Ion-solid interaction alters the topography of solid surfaces via competing surface roughening and smoothing processes. These competing processes are responsible for the creation of surface features like quasiperiodic ripple [8, 9, 10, 11] and self-affine fractal topographies [3, 4, 5, 11]. In the ion mass-energy regime where sputtering is dominant, surface roughening is observed [3, 4, 11]. When ion-beam induced effective surface diffusion dominates surface smoothing is observed [5, 9, 12]. The smoothed surface can also be a self-affine fractal surface [5].

Surface morphology is often described by some statistical parameters. Most common are the surface width (σ), represented by the root-mean-square roughness value, and the in-plane correlation length (ξ). The correlation length is the average distance between features in the surface profiles within which the surface variations are correlated. Surface width is an important parameter that represents a measurement of the correlations along the direction of the surface growth. Scaling studies can be performed by measuring surface roughness at various length scales. Root-mean-square surface roughness σ is

*bhupen@iopb.res.in

defined as

$$\sigma =< [h(x,y) - h]^2 >^{1/2}, \quad (1)$$

where $h(x, y)$ is the surface height at a point (x, y) on the surface and h is the average height. If the horizontal sampling length on the surface is L and $\sigma \propto L^{\alpha}$, where $0 < \alpha < 1$, the surface is termed self-affine [4]. The value of the scaling exponent α indicates how roughness changes with length scales. However, it does not tell whether the surface is roughened or smoothed upon any kind of surface treatment. Small α values are associated with jagged surfaces (anticorrelation) while large values indicate well correlated, smoothed-textured surfaces. The surface width (rms roughness) scales with linear length L for $L << \xi$ and for $L >> \xi$ rms roughness $\sigma(L) \rightarrow \sigma_0$. For the case $\xi >> a$ (lattice spacing of the system) the analytical form of roughness can be written as [13]:

$$\sigma^2(L) = \frac{\sigma_0^2}{(1 + 4\pi\xi^2/2\alpha L^2)^{\alpha}} \quad (2)$$

In ion-surface interaction, in a previous work we observed ion-beam induced surface smoothing and the smoothed surface to be self-affine. 2.0 MeV Si^+ ions bombarded on a Si(100) surface (hereafter denoted IB) with the fluences in the range $10^{15} - 10^{16}$ ions/cm^2, produced a self-affine fractal surface with a scaling exponent $\alpha = 0.53 \pm 0.03$ at length scales below 50 nm [5]. In ion-atom collisions in solids and at the surface, the elastic energy lost by an ion is transferred to a recoil atom, which itself collides with other atoms in the solid and so forth. In this way the ion creates what is called a collision cascade. The displaced atoms in this collision cascade may acquire a kinetic energy enough to escape from the solid surface − a phenomenon known as sputtering. However, if the energy (component normal to the surface) of the displaced atoms is smaller than the surface binding energy, the atoms may reach the surface but cannot leave the surface. They can, however, drift parallel to the surface providing an effective surface diffusion. Apparently this ion-beam induced effective surface diffusion causes nanometer-scale surface smoothing [5]. Discovery of this ion-irradiation induced nanoscale surface smoothing phenomenon leading to a self-affine fractal surface inspired further investigations [14] including the present one.

In surface studies and epitaxial thin film growth, thermal treatment of the solid substrate is almost inevitable. Thermal treatment of ion-bombarded surfaces (hereafter denoted TIB) produced a self-affine surface with a different roughness exponent with both smoothing and roughening below and above a particular length scale, respectively. At length scales below $\sim$ 50 nm, thermal treatment was found to cause further smoothing of the ion-bombardment induced smooth surface (IB). However, at length scales above $\sim$ 50 nm the surface roughness of the TIB samples increases for lateral dimensions upto $\sim$ 300 nm with a scaling exponent $\alpha = 0.81 \pm 0.04$ over the entire range covering both smoothing and roughening regimes [14]. Scaling studies for Ge growth on this surface as well as on the pristine Si(100) surface are reported here.

Another motivation for the study of growth of Ge on ion-irradiated Si surfaces is related to our earlier studies of growth of Ge nanostructures on silicon [15, 16]. Growth of Ge nanodots and nanowires on polymer-coated Si surfaces indicated that nanodots are arranged on defects, which might be utilized to fabricate lattices of nanodots. Patterned defect structures can be created on Si by ion-irradiation. Ge growth on this patterned surface could possibly be used to form Ge nanodot lattices. However, these aspects will not be presented here.

II. EXPERIMENTAL

Si(100) substrates with the native oxide were irradiated with 2.0 MeV Si^+ ions. The ion beam was incident along the surface normal ($\theta \approx 0°$) and rastered on the sample in order to obtain a uniformly irradiated area. One half of the sample was masked and hence unirradiated. An ion beam flux of $\approx 1 \times 10^{12}$ cm^{-2} sec^{-1} was used with a fluence of 4×10^{15} ions/cm^2. The pressure in the irradiation chamber was $\sim 10^{-7}$ mbar. Following irradiation the sample was taken out and inserted into an ultrahigh vacuum (UHV) chamber (pressure: 3×10^{-10} mbar) containing an Omicron variable temperature scanning tunneling microscope. Scanning tunneling microscopy (STM) measurements were performed at room temperature. The roughness measurements were made on both the pristine as well as the irradiated half of the sample with a thin ($\sim$ 1.5 nm) native oxide layer. For preparing a clean silicon surface, the sample was degassed about 600°C for 12 hours prior to the flashing at 1200°C for 2−3 minutes under UHV condition (1×10^{-10} mbar) in a molecular beam epitaxy (MBE) growth chamber. This process removes the native oxide and exposes a clean Si surface. The MBE and the STM chambers are connected. This system is described in ref [17] On the clean pristine half of the sample we observe surface atomic steps as usually observed on the atomically clean Si(100) surfaces. Roughness measurements were again made on both the pristine and the ion-irradiated halves of the sample after removal of the oxide. Roughness exponents were determined from STM images. A large number of scans, each of size L, were recorded on the surface at random locations. The σ values for the rms roughness given by the instrument plane fitting and subtraction procedure had been carried out. This procedure was repeated for many different sizes and a set of average σ versus L values was obtained. On the entire clean (oxide removed) surface, having performed scaling measurements, $\sim 6\mathring{A}$ Ge was deposited while the substrate was kept at 550°C (the standard condition for Ge epitaxy on silicon). Scaling measurements on both halves have been made again following Ge deposition.

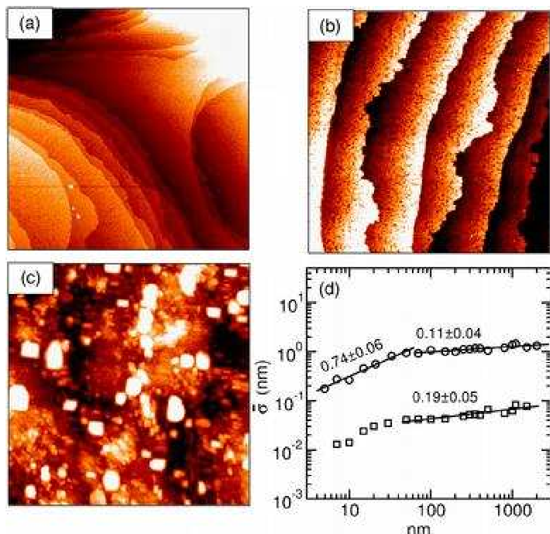

FIG. 1: STM images (a) (1500×1500 nm^2) and (b) (300×300 nm^2) of a clean pristine Si(100) surface. Atomic steps and terraces are seen. (c) A STM image (400×400 nm^2) of a Ge-deposited film on Si(100). (d) Average rms surface roughness ($\bar{\sigma}$) vs scan size (L) on the pristine Si(100) [□,TP] and on the Ge-deposited pristine surface [○,TP+Ge] surfaces. The values of the roughness exponents α are shown in Fig.1(d).

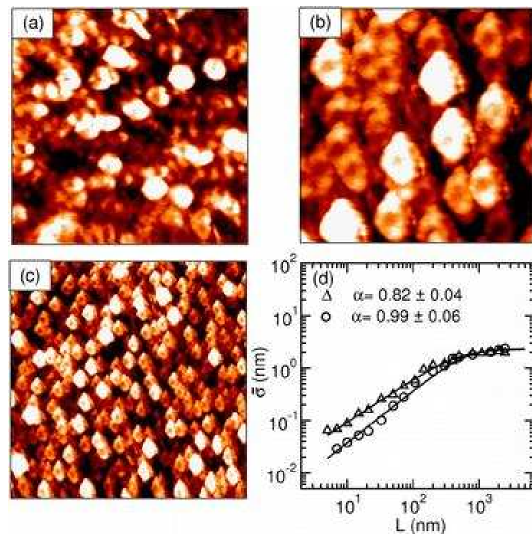

FIG. 2: (a) A STM image (1100×1100 nm^2) of an ion-irradiated cleaned (TIB) Si(100) surface. STM images (b) (1100×1100 nm^2) and (c) (3000×3000 nm^2) from the Ge-deposited (TIB+Ge) surface. (d) Average roughness ($\bar{\sigma}$) vs scan size (L) plots: for the TIB [△] surface and the TIB+Ge [○] surface. Roughness exponents are marked in the figure.

III. RESULTS AND DISCUSSIONS

A. Ge deposition on the pristine surface

The pristine half of the Si(100) surface shows the typical (2×1) reconstruction [This sample will be referred to thermally treated pristine, TP]. STM images [Fig.1(a),(b)] show flat terraces and atomic steps. Ge deposition on the pristine surface leads to Ge island growth [Fig.1(c)]. Ge is known to grow on Si in the Stranski-Krastanov or layer-plus-island mode. The results of roughness scaling studies on the clean Si(100) surface as well as on the Ge-deposited surface are shown in Fig.1(d). For length scales >50 nm roughness exponents are found to be 0.19 ± 0.05 and 0.11 ± 0.04 for the clean Si(100) and the Ge-deposited Si(100) surface, respectively. $\alpha\rightarrow0$ corresponding to local dimension D=$3-\alpha\rightarrow3$, is a subtle situation, since a three dimensional object can be either a fractal or a volume. As we notice, clean surface is dominated by (100) terraces with monatomic steps [Fig.1(b)]. At larger length scales multiple steps with short terraces or step bunching are encountered; this tends to increase the roughness values. Roughness values are very small (~0.05 nm). Upon Ge deposition, the value of roughness increases more than an order of magnitude, however the roughness exponent does not change significantly. Roughness exponent observed here is quite small. Observation of such a small value of α (0.12 ± 0.05) was earlier reported for roughness on a Ag film deposited by thermal evaporation on a polished quartz crystal [13]. For the Ge film, surface is smoother at length scales <50 nm with the roughness exponent $\alpha=0.74\pm0.06$. Assuming that the knee regime in the $\sigma(L)$ plot corresponds to a length scale approximately 4ξ, for the Ge-deposited surface the in-plane correlation length ξ is $\sim$12 nm.

B. Ge deposition on the ion-irradiated surface

Surface morphology of an ion-irradiated clean Si(100) surface is seen in the STM image of Fig.2(a). Fig.2(b) and Fig.2(c) show STM micrographs following Ge deposition. These are quite different from that for Ge deposition on a pristine Si(100) surface. Nearly diamond shaped islands are seen in Fig.2(b) and Fig.2(c), while dominant square or rectangular shaped islands are seen in Fig.1(c). An ideal Si(100) surface has a fourfold symmetry, while the (2×1) reconstructed Si(100) surface has a twofold symmetry. These dictate the square or rectangular island shape. On the irradiated clean Si(100) surface, neither large terraces nor (2×1) reconstruction is observed. The log-log plots of average surface roughness ($\bar{\sigma}$) versus scan size L are shown in Fig.2(d). Above the length scales of $\sim$700 nm both the surfaces practically have the same roughness. That is, the Ge deposition has hardly any effect on the saturation roughness, σ_0, at these length scales. However, for length scales below 700 nm, Ge-deposited surface shows considerable surface smoothing than the TIB surface. From the linear portion of the log $\bar{\sigma}$ versus log L plot the roughness scaling exponents have been found as 0.82 ± 0.04 for the TIB surface and 0.99 ± 0.06 for the Ge-deposited surface. This indicates

TABLE I: Roughness exponent (α) and the in-plane correlation length (ξ)

Sample	α	ξ (nm)
TP Si(100)	0.19±0.05	–
TP Si(100)+Ge	0.11±0.04	–
	0.74±0.06	~ 12
IB Si(100)	0.53±0.03[a]	–
TIB Si(100)	0.82±0.04[b]	32±3.0
TIB + Ge	0.99±0.06	137±10.0

[a]from Ref.[5]
[b]from Ref.[14] and the present study

that both the surfaces are self-affine fractal in nature.

Fits using Eq.(2) are also shown in Fig.2(d). We have used the values of α in Eq.(2) from the fitting of the linear portion of the curve in the log-log plot. The results are presented in Table-1.

As discussed in ref[14] thermal treatment of the ion-irradiated Si(100) surface (TIB) simultaneously smoothes and roughens the surface at different length scales, with the same roughness exponent over the entire length scales. Ge deposition causes further smoothing over this entire region [Fig.2(d)] with an increased in-plane correlation length. The correlation length ξ, together with the roughness exponent α, controls how far a point on the surface can move before losing the memory of the initial value of its height (h) coordinate.

After removal of the native oxide by thermal treatment, the roughness of the irradiated (TIB) surface is found to be much larger compared to the pristine (TP) surface. The reason for this has been explained in ref.[14] by Monte Carlo simulation results showing atomic displacements at the ion-bombarded oxide/Si interface. The loss of symmetry and the new structure formation on the TIB surface is apparently responsible for the difference in morphology of the Ge-deposited surfaces in Fig.1(c) and Fig.2(b) [also Fig.2(c)]. The difference in morphologies of the clean surfaces as seen in Fig.1(a) [also Fig.1(b)] and Fig.2(a) would lead to a difference in adhesion of deposited atoms on them. The smoothing observed at smaller length scales upon Ge-deposition on the TIB surface indicates that the Ge atoms fill the surface troughs, where the deposited atoms would have more nearest neighbors for better bonding. [For length scales ≤ 200 nm the Ge-deposited TIB surface is also smoother than the Ge-deposited TP surface]. The theoretical work of Palasantzas and Hosson [7] predicting that the adhesion of a thin film deposited on a fractal surface would depend on the fractal dimension of the substrate surface needs to be further explored through experimental investigations.

Considering the fact that the ion-irradiation was performed at $\sim 10^{-7}$ mbar, one may wonder about deposition of C on the irradiated surface and its influence on subsequent results. However, we do not expect any significant C deposition. This aspect has been explained in details in ref. [5].

IV. SUMMARY AND CONCLUSIONS

Roughness scaling behavior of thin Ge films on ion-irradiated and pristine Si(100) surfaces has been investigated. Ge was deposited after removal of the native oxide under ultrahigh vacuum condition. On the pristine surface, upon Ge deposition, although the roughness increases more than an order of magnitude the roughness exponent α changes from 0.19 to 0.11. On the ion-irradiated surface, Ge deposition causes surface smoothing with roughness exponent changing from 0.82 to 0.99. In these two cases, different fractal dimensions of the fractal surfaces of the substrates, 2.81 for the pristine and 2.18 for the ion-irradiated, has apparently led to different surface morphologies of the Ge-deposited surfaces. Ge islands on the pristine surface tend to have square or rectangular shape, while the islands on the ion-irradiated surface have nearly diamond shaped structures. For metal films on semiconductors, recently interesting island structures with quantized heights − apparently an effect of electronic confinement − have been observed [18, 19, 20]. This type of growth cannot be explained within the traditional FM, SK and VW growth modes. Recent theoretical models indicate an *electronic growth* mechanism for such systems, where energy contribution of the quantized electrons confined in the metal overlayer can actually determine the morphology of the growing film [21]. The electronic structure of these islands would depend on their shape. The possibility of influencing the shape of the islands by growth on surfaces of different fractal dimensions would provide the capability of manipulating the electronic behavior of such nanostructures.

[1] B. B. Mandelbordt, The Fractal Geometry of Nature (Freeman, New York, 1982).

[2] R. Chiarello, V. Panella, J. Krim and C. Thompson, Phys. Rev. Lett. 67 (1991) 3408; C. Thompson, G. Palasantzas, Y. P. Feng, S. K. Sinha and J. Krim, Phys. Rev. B 49 (1994) 4902.

[3] E. A. Eklund, R. Bruinsma, J. Rudnick, and R. S. Williams, Phys. Rev. Lett. 67 (1991) 1759.

[4] J. Krim, I. Heyvart, D. V. Haesendonck, and Y. Bruynseraede, Phys. Rev. Lett. 70 (1993) 57.

[5] D. K. Goswami and B. N. Dev, Phys. Rev. B 68 (2003) 033401-1.

[6] E. Bauer and J. H. van der Merwe, Phys. Rev. B 33 (1986) 3657

[7] G. Palasantzas and J. Th. M. De Hosson, Phys. Rev. E 67 (2003) 021604.

[8] E. Chason, T. M. Mayer, B. K. Kellerman, D. T. McIlroy and A. J. Howard, Phys. Rev. Lett. 72 (1994) 3040.

[9] G. Carter and V. Vishnayakov, Phys. Rev. B 54 (1996) 17647.

[10] For a review, see K. Wittmaack, in Practical Surface Analysis, Vol.2, Ion and Neutral Spectroscopy, edited by D. Briggs and M. P. Seah (Wiley, Chichester, 1992) chap.3, p.122.

[11] S. Habenicht, W. Bolse, K. P. Lieb, K. Reimann, and U. Geyer, Phys. Rev. B 60 (1999) R2200.

[12] S. G. Mayr and R. S. Averback, Phys. Rev. Lett. 87 (2001) 196106.

[13] G. Palasantzas, Phys. Rev. B 48 (1993) 14472.

[14] D. K. Goswami and B. N. Dev, Nucl. Inst. Meth. Phys. Res. B 212 (2003) 235.

[15] Amal K. Das, S. K. Ghose, B. N. Dev, G. Kuri and T. R. Yang, Appl. Surf. Sci. 165 (2000) 260.

[16] Amal K. Das, J. Kamila, B. N. Dev, B. Sundaravel and G. Kuri, Appl. Phys. Lett. 77 (2000) 951; Appl. Phys. Lett. 78 (2001) 3552.

[17] D. K. Goswami, B. Satpati, P. V. Satyam and B. N. Dev, Curr. Sci. 84 (2003) 903.

[18] L. Gavioli, K. R. Kimberlin, M. C. Tringides, J. F. Wendelken and Z. Zhang, Phys. Rev. Lett. 82 (1999) 129.

[19] D. K. Goswami, K. Bhattacharjee, B. Satpati, S. Roy, G. Kuri, P. V. Satyam and B. N. Dev, cond-mat/0311506, Phys. Rev. B (submitted).

[20] W. B. Su, S. H. Chang, W. B. Jian, C. S. Chang, L. J. Chen and T. T. Tsong, Phys. Rev. Lett. 86 (2001) 5116.

[21] Z. Y. Zhang, Q. Niu and C.-K. Shih, Phys. Rev. Lett. 80 (1998) 5381; Z. G. Suo and Z. Y. Zhang, Phys. Rev. B 58 (1998) 5116; H. Okamoto, D. Chen and T. Yamada, Phys. Rev. Lett. 89 (2002) 256101-1; C. M. Wei and M. Y. Chou, Phys. Rev. B68 (2003) 125406; Phys. Rev. B 66 (2002) 233408.